Revista EIA, ISSN 1794-1237 Número 2 p. 75-88. Agosto 2004
Escuela de Ingeniería de Antioquia, Medellín (Colombia)

FRICTIONLESS CONTACT IN A LAYERED PIEZOELECTRIC MEDIUM COMPOSED OF MATERIALS WITH HEXAGONAL SYMMETRY

GUILLERMO RAMIREZ*

ABSTRACT

A matrix formulation is presented for the solution of frictionless contact problems on arbitrarily multilayered piezoelectric half-planes. Different arrangements of elastic and transversely orthotropic piezoelectric materials within the multilayered medium are considered. A generalized plane deformation is used to obtain the governing equilibrium equations for each individual layer. These equations are solved using the infinite Fourier transform technique. The problem is then reformulated using the local/global stiffness method, in which a local stiffness matrix relating the stresses and electric displacement to the mechanical displacements and electric potential in the transformed domain is formulated for each layer. Then it is assembled into a global stiffness matrix for the entire half-plane by enforcing interfacial continuity of tractions and displacements. This local/global stiffness approach not only eliminates the necessity of explicitly finding the unknown Fourier coefficients, but also allows the use of efficient numerical algorithms, many of which have been developed for finite element analysis. Unlike finite element methods, the present approach requires minimal input. Application of the mixed boundary conditions reduces the problem to an integral equation. This integral equation is numerically solved for the unknown contact pressure using a technique based on the Chebyshev polynomials.

KEY WORDS: piezoelectricity; contact pressure; multilayered half-plane.

RESUMEN

Se presenta una formulación matricial para la solución de problemas de contacto sin fricción en semiplanos piezoeléctricos elásticos de múltiples capas. Se consideran diferentes disposiciones de materiales piezoeléctricos elásticos y transversalmente ortotrópicos dentro del medio de múltiples capas. Se usa una deformación de plano generalizada para obtener las ecuaciones gobernantes de equilibrio para cada capa individual, que se resuelven con la técnica de transformada de Fourier infinita. Entonces el problema se reformula con el método de rigidez local/global, en el cual se formula para cada capa una matriz de rigidez local que relaciona los esfuerzos y el desplazamiento eléctrico con los desplazamientos mecánicos y el potencial eléctrico en el dominio transformado. En seguida se ensambla en una matriz de rigidez global para todo el semiplano imponiendo la continuidad interfacial de tracciones y desplazamientos. Este enfoque por rigidez local/global no sólo elimina la necesidad de hallar explícitamente los coeficientes de Fourier desconocidos, sino que también permite el uso de algoritmos numéricos eficientes, muchos de los cuales se desarrollaron para análisis por elementos finitos. A diferencia de los métodos de elementos finitos, este enfoque requiere una entrada miníma. El uso de condiciones de borde mezcladas reduce el problema a una ecuación integral, que se resuelve para la presión de contacto desconocida con una técnica basada en los polinomios de Chebyshev.

PALABRAS CLAVE: piezoelectricidad; presión de contacto; semiplano de varias capas.

---

* Ingeniero Civil. Ph. D. Department of Civil and Environmental Engineering. Tennessee Technological University. Cookeville, Tennessee 38505

Artículo recibido 19-IV-2004. Aprobado con revisión 3-VIII-2004.
Discusión abierta hasta enero 2005.

1. INTRODUCTION

The study and analysis of layered smart media (also referred to as intelligent or adaptive) have received considerable attention in recent years. This is in part because of their potential applicability as sensors and actuators for sensing and controlling the response of structures to a changing environment. These materials have the ability of converting energy from one form (among magnetic, electric, and mechanical energies) to other. As with other deformable solids, the phenomenon of contact can provide critical information related to design and performance of structural components constructed in part using these materials. The use of piezoelectric layers or elements as a pressure sensor is one of many types of applications for this type of problem. In this context, the sensor application could then be combined with the actuator application to design an active loop to control the deformation and shape of the host structure subjected to contact pressure.

Contact problems in elasticity have a large and varied history as seen, for example, in Gladwell. The extensions to the effects of piezoelectric materials, however, have not yet been made to any great extent. In the present work, we apply the local/global technique originally developed for elastic contact problems by Pindera and Lane in 1993, in which the response of layered half-planes was analyzed within the framework of the generalized plane deformation formulation. The local/global procedure is based on the transfer and flexibility matrix formulation presented by Bufler in 1971 for isotropic layered media with constant elastic properties, later reformulated in terms of the local stiffness matrix by Rowe and Booker in 1982 and applied to non-homogeneous isotropic layered soils. The local/global stiffness approach facilitates decomposition of the integral equation for the contact stress distribution on the top surface of the layered half-plane into singular and regular parts, that in turn, can be numerically solved by using the collocation technique outlined by Erdogan.

In this study, we apply a similar type of formulation to consider the influence of contact pressure on contact length for typical piezoelectric solids, and determine typical surface and sub-surface distributions for the electric fields under the conditions of frictionless contact.

2. FORMULATION

2.1 Geometry

A multilayered medium composed of an arbitrary arrangement of elastic and/or piezoelectric laminae bonded to a homogeneous elastic or piezoelectric half-plane is considered in the present study. The layered medium is infinite in the $x\,y$-plane and the loading on the top surface is assumed to be independent of the y-coordinate, allowing the problem to be formulated as a planar problem in the xy-coordinate system that it is also infinite. The variables u, v, and w represent the mechanical displacements in the x–, y–, and z– directions, respectively, and ϕ represents the electrostatic potential. The assemblage is indented by a rigid, frictionless punch of a parabolic profile. The corresponding configuration is shown in Figure 1.

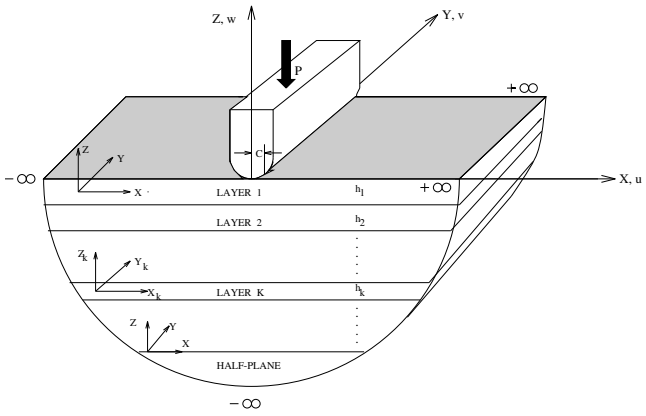

Figure 1. Geometry and layer configuration

2.2 Governing equations

The theory of linear piezoelectricity has been used throughout this study. Accordingly, the constitutive equations that describe the electro-mechanical coupling phenomenon are given by

$$\sigma_{ij} = C_{ijkl} S_{kl} - e_{kij} E_k$$

$$D_i = e_{ikl} S_{kl} + \varepsilon_{ik} E_k \tag{1}$$

where σ_{ij} are the components of the stress tensor, e_{kij} are the components of the piezoelectric constants of the solid, ε_{ik} are the components of the dielectric tensor, C_{ijkl} are the components of the elastic stiffness tensor, E_k represent the electric field, and S_k are the components of the infinitesimal strain tensor.

The equations of equilibrium and the Gauss equation of electricity in the absence of electric charges and current densities are given by

$$\sigma_{ij,j} + f_i = 0 \tag{2}$$

and

$$D_{i,i} = 0, \tag{3}$$

respectively. Here f_i are the components of the body force and D_i represent the electric displacement components. Auxiliary equations are needed to relate the strain and the electric fields to the displacement and electrostatic potential fields, respectively. Those relations are given by the mechanical strain-displacement equations

$$S_{ij} = \frac{1}{2}\left(u_{i,j} + u_{j,i}\right) = \frac{1}{2}\left(\frac{\partial u_j}{\partial x_i} + \frac{\partial u_i}{\partial x_j}\right) \tag{4}$$

and the electric field-electrostatic potential equations

$$E_i = -\phi_{,i} = -\frac{\partial \phi}{\partial x_i} \tag{5}$$

where u_i represent the displacement components (u in the x–, v in the y–, and w in the z– directions) and ϕ represents the electric potential.

The equations of equilibrium and conservation of electrostatic charge (Gauss equation of electricity) for an orthotropic material oriented off-axis may be expressed in terms of the mechanical displacements and the electrostatic potential as

(6)

here $(\,)_{,x}$ represents and represents . The above equations are reduced for an orthotropic material oriented on-axis as follows

$$C_{11}u_{,xx} + C_{55}u_{,zz} + (C_{13} + C_{55})w_{,xz} + (e_{31} + e_{15})\phi_{,xz} = 0$$

(7)

The solution of Equations (6) and (7) for each layer must satisfy the external surface boundary conditions as well as the continuity of stresses σ_{xz}, σ_{yz}, σ_{zz}, electric displacement D_z, electric potential ϕ, and mechanical displacements u, v, and w. The external surface mixed boundary conditions are expressed as

(8)

and the continuity conditions are given by

$$D_z^k(x, -h_k/2) = D_z^{k+1}(x, h_{k+1}/2) \tag{9}$$

Here represent the displacements and potential at the top or bottom interface of a given layer k, and and D_z^k are the stresses and electric displacement at the upper or lower interfaces of the layer in consideration.

A Fourier transform technique is used to solve the system of Equations (6) and (7). Consequently, by transforming these equations, the equilibrium and electrostatic charge expressions for an orthotropic off-axis layer may be written as

$$\begin{aligned}
&-\xi^2 C_{16}\bar{U} + C_{45}\bar{U}_{,zz} - \xi^2 C_{66}\bar{V} + C_{44}\bar{V}_{,zz} - i\xi(C_{36} + C_{45})\bar{W}_{,z} - i\xi(e_{36} + e_{14})\bar{\Phi}_{,z} = 0\\
&-i\xi(C_{13} + C_{55})\bar{U}_{,z} - i\xi(C_{36} + C_{45})\bar{V}_{,z} - \xi^2 C_{55}\bar{W} + C_{33}\bar{W}_{,zz} - \xi^2 e_{15}\bar{\Phi} + e_{33}\bar{\Phi}_{,zz} = 0\\
&-i\xi(e_{15} + e_{31})\bar{U}_{,z} - i\xi(e_{14} + e_{36})\bar{V}_{,z} - \xi^2 e_{15}\bar{W} + e_{33}\bar{W}_{,zz} + \xi^2 \varepsilon_{11}\bar{\Phi} - \varepsilon_{33}\bar{\Phi}_{,zz} = 0
\end{aligned} \tag{10}$$

where ξ is the transform variable and an overbar indicates a transformed quantity. For brevity, the transformed equations for on-axis orthotropic materials are omitted.

The solution to Equations (10) in the transformed domain is sought in the form

$$\bar{W}(\xi,z)=\bar{W}_o(\xi)\,e^{\xi\lambda z} \qquad \bar{U}(\xi,z)=\bar{U}_o(\xi)\,e^{\xi\lambda z}$$
$$\bar{V}(\xi,z)=\bar{V}_o(\xi)\,e^{\xi\lambda z} \qquad \bar{\Phi}(\xi,z)=\bar{\Phi}_o(\xi)\,e^{\xi\lambda z} \tag{11}$$

where $\bar{W}_o(\xi)$, , , and are the unknown Fourier coefficients. By substituting these assumed solutions into the transformed equilibrium and electrostatic charge expressions, Equations (10), the following matrix system is obtained for the orthotropic off-axis lamina

$$\begin{bmatrix} (C_{11}-\lambda^2 C_{55}) & (C_{16}-\lambda^2 C_{45}) & i\lambda(C_{13}+C_{55}) & i\lambda(e_{31}+e_{15}) \\ (C_{16}-\lambda^2 C_{45}) & (C_{66}-\lambda^2 C_{44}) & i\lambda(C_{36}+C_{45}) & i\lambda(e_{36}+e_{14}) \\ i\lambda(C_{13}+C_{55}) & i\lambda(C_{36}+C_{45}) & (C_{55}-\lambda^2 C_{33}) & (e_{15}-\lambda^2 e_{33}) \\ i\lambda(e_{31}+e_{15}) & i\lambda(e_{36}+e_{14}) & (e_{15}-\lambda^2 e_{33}) & (\lambda^2\varepsilon_{33}-\varepsilon_{11}) \end{bmatrix} \begin{Bmatrix} \bar{U}_o(\xi) \\ \bar{V}_o(\xi) \\ \bar{W}_o(\xi) \\ \bar{\Phi}_o(\xi) \end{Bmatrix} = \begin{Bmatrix} 0 \\ 0 \\ 0 \\ 0 \end{Bmatrix} \tag{12}$$

For this system of homogeneous equations to have a nontrivial solution, it is necessary to set the determinant of the matrix equal to zero. The solution of the resulting equation gives the eigenvalues or characteristic roots λ. In the case of a piezoelectric monoclinic material, there are eight eigenvalues λ and eight unknown Fourier coefficients, , , and , for each layer. This shows the coupling among all three mechanical displacements and the electrostatic potential. Materials such as PVDF exhibit orthotropic material symmetry and normally generate only real or imaginary roots (Heyliger and Brooks[6] and Ramirez and Heyliger[7]). The form for the displacements in this case can be written in terms of hyperbolic sine and cosine functions and are shown elsewhere (Ramirez and Heyliger[7]). Materials that have hexagonal symmetry can generate two pairs of conjugate complex roots and a pair of real roots. The complex roots may be expressed as $a\pm ib$ and $-a\pm ib$. The displacement V uncouples from the other displacements and electric potential for materials that exhibit this hexagonal symmetry.

Once the eigenvalues are found, the unknown Fourier coefficients $\bar{V}_o$, , and are written in terms of from Equation (12). After some mathematical manipulations, the contributions to the displacements and electrostatic potential may be written in terms of the trigonometric and hyperbolic functions as follows

$$\frac{\bar{W}}{i}=\sinh(\xi az)[(C_{A1}F_2+C_{A2}G_1)\cos(\xi bz)+(-C_{A2}F_1+C_{A1}G_2)\sin(\xi bz)]+$$

(13)

where C_{A1}, C_{A2}, C_{B1}, and C_{B2} are constants that depend on the geometry, material properties, and the complex eigenvalues λ. Similarly, expressions for the stresses and the electric displacement can be obtained using appropriate differentiation and constitutive laws, and are given by

$$\frac{\bar{D}_z(\xi, z)}{i\xi} =$$

(14)

where

2.3 Local/global matrix

In order to reduce the contact problem to a singular integral equation for the unknown pressure distribution along the contact area, the problem is restated in terms of the interfacial displacements along the common interfaces separating the individual layers instead of the unknown Fourier coefficients F_j and G_j. Through this procedure, it is possible to construct a local stiffness matrix for each layer relating the lamina stresses and electric displacement at upper and lower surfaces of each layer to the corresponding mechanical displacements and electrical potential. First the stresses are written in terms of the Fourier coefficients as

$$
\begin{aligned}
f_1 &= -C_{13} + C_{33}(a\,C_{A1} - b\,C_{A2}) + e_{33}(a\,C_{B1} - b\,C_{B2}) \\
f_2 &= C_{33}(a\,C_{A2} + b\,C_{A1}) + e_{33}(a\,C_{B2} + b\,C_{B1}) \\
g_1 &= C_{55}(a + C_{A1}) + e_{15}C_{B1} \\
g_2 &= C_{55}(b + C_{A2}) + e_{15}C_{B2} \\
h_1 &= -e_{31} + e_{33}(a\,C_{A1} - b\,C_{A2}) - \varepsilon_{33}(a\,C_{B1} - b\,C_{B2}) \\
h_2 &= e_{33}(a\,C_{A2} + b\,C_{A1}) - \varepsilon_{33}(a\,C_{B2} + b\,C_{B1}) \\
Q_4 &= \lambda_4 C_{44}
\end{aligned}
$$

$$
\begin{Bmatrix}
\dfrac{\bar{\sigma}_{zz}^{+}}{\xi i} \\[2ex]
\dfrac{\bar{\sigma}_{xz}^{+}}{\xi} \\[2ex]
\dfrac{\bar{D}_{z}^{+}}{\xi i} \\[2ex]
\dfrac{-\bar{\sigma}_{zz}^{-}}{\xi i} \\[2ex]
\dfrac{-\bar{\sigma}_{xz}^{-}}{\xi} \\[2ex]
\dfrac{-\bar{D}_{z}^{-}}{\xi i}
\end{Bmatrix}
=
\begin{bmatrix}
f_1 s_h c_s & f_1 c_h s_n & P_3 s_{h3} & f_1 c_h c_s & f_1 s_h s_n & P_3 c_{h3} \\
-f_2 c_h s_n & +f_2 s_h c_s & & -f_2 s_h s_n & +f_2 c_h c_s & \\
g_1 c_h c_s & g_1 s_h s_n & T_3 c_{h3} & g_1 s_h c_s & g_1 c_h s_n & T_3 s_{h3} \\
-g_2 s_h s_n & +g_2 c_h c_s & & -g_2 c_h s_n & +g_2 s_h c_s & \\
h_1 s_h c_s & h_1 c_h s_n & X_3 s_{h3} & h_1 c_h c_s & h_1 s_h s_n & X_3 c_{h3} \\
-h_2 c_h s_n & +h_2 s_h c_s & & -h_2 s_h s_n & +h_2 c_h c_s & \\
f_1 s_h c_s & f_1 c_h s_n & P_3 s_{h3} & -f_1 c_h c_s & -f_1 s_h s_n & -P_3 c_{h3} \\
-f_2 c_h s_n & +f_2 s_h c_s & & +f_2 s_h s_n & -f_2 c_h c_s & \\
-g_1 c_h c_s & -g_1 s_h s_n & -T_3 c_{h3} & g_1 s_h c_s & g_1 c_h s_n & T_3 s_{h3} \\
+g_2 s_h s_n & -g_2 c_h c_s & & -g_2 c_h s_n & +g_2 s_h c_s & \\
h_1 s_h c_s & h_1 c_h s_n & X_3 s_{h3} & -h_1 c_h c_s & -h_1 s_h s_n & -X_3 c_{h3} \\
-h_2 c_h s_n & +h_2 s_h c_s & & +h_2 s_h c_s & -h_2 c_h c_s &
\end{bmatrix}
\begin{Bmatrix}
F_1 \\ G_2 \\ G_3 \\ F_2 \\ G_1 \\ F_3
\end{Bmatrix}
\tag{15}
$$

Secondly, and in similar way as that for the stresses, the displacements and electrostatic potential are also evaluated at $\pm\frac{h}{2}$ to yield

(16)

and

$$\begin{Bmatrix} \dfrac{\bar{W}^{+}-\bar{W}^{-}}{2i} \\ \dfrac{\bar{U}^{+}+\bar{U}^{-}}{2} \\ \dfrac{\bar{\Phi}^{+}-\bar{\Phi}^{-}}{2i} \end{Bmatrix} = \begin{bmatrix} C_{A1}\,s_h\,c_s - C_{A2}\,c_h\,s_n & C_{A2}\,s_h\,c_s + C_{A1}\,c_h\,s_n & R_3\,s_{h3} \\ c_h\,c_s & s_h\,s_n & c_{h3} \\ C_{B1}\,s_h\,c_s - C_{B2}\,c_h\,s_n & C_{B2}\,s_h\,c_s + C_{B1}\,c_h\,s_n & S_3\,s_{h3} \end{bmatrix} \begin{Bmatrix} F_2 \\ G_1 \\ F_3 \end{Bmatrix} \tag{17}$$

where the following symbols have been used

$$c_{hj} = \cosh\left(\xi\,\lambda_j\,\frac{h}{2}\right)$$
$$c_h = \cosh\left(\xi\,a\,\frac{h}{2}\right)$$
$$c_s = \cos\left(\xi\,b\,\frac{h}{2}\right)$$

where the ± superscripts refer to the top and bottom surfaces of each layer. Using matrix operations, it is possible to solve for the Fourier coefficients F_j and G_j in terms of the displacements and the electrical potential in Equations (16) and (17) and then substitute them into Equation (15). This mathematical procedure yields the local coefficient matrix that relates the mechanical displacements and electrical potential to the transverse stresses and electrical displacement at the top and bottom of each layer. The result can be symbolically written as

(18)

where and $\{T\}_k^{\pm} = \{\bar{\sigma}_{zz}^{\pm} / i\xi, \bar{\sigma}_{xz}^{\pm} / i\xi,$

Imposition of the interfacial conditions on mechanical displacements, potential, stresses, and normal electric displacement along the common interfaces,

$$\begin{aligned} \{\bar{U}\}_{k+1}^{+} &= \{\bar{U}\}_k^{-} = \{\bar{U}\}_{k+1} \\ & \qquad \text{for } k = 1, \ldots, (n-1) \\ \{\bar{T}\}_{k+1}^{k} + \{\bar{T}\}_k^{-} &= 0 \end{aligned}$$

together with the external boundary conditions yields a system of equations where the interfacial displacement components and the electrostatic potential are the only unknowns. This global system can be expressed as

$$\begin{bmatrix} [K]_{11}^{1} & [K]_{12}^{1} & 0 & \cdots & 0 \\ [K]_{21}^{1} & [K]_{22}^{1} + [K]_{11}^{2} & [K]_{12}^{2} & \cdots & \vdots \\ 0 & [K]_{21}^{2} & [K]_{22}^{2} + [K]_{11}^{3} & \cdots & \vdots \\ 0 & 0 & [K]_{21}^{3} & \ddots & \vdots \\ 0 & 0 & \cdots & \cdots & [K]_{22}^{*n-1} + [K]_{11}^{*n} \end{bmatrix} \begin{Bmatrix} \{\bar{U}\}_1 \\ \{\bar{U}\}_2 \\ \vdots \\ \vdots \\ \{\bar{U}\}_n \end{Bmatrix} = \begin{Bmatrix} \{\bar{T}\}_1^{+} \\ \{0\} \\ \vdots \\ \vdots \\ \{0\} \end{Bmatrix}. \tag{19}$$

By enforcing the continuity of displacements and potential along the interfaces of the layered medium, the redundant continuity equations are eliminated. This results in a reduction in the total number of unknowns in the system.

$$w_{,x}^{1} = \frac{-1}{\sqrt{2\pi}} \int_{-\infty}^{+\infty} H_{(1,1)}(\xi) \left(\frac{1}{\sqrt{2\pi}} \int_{-c}^{+c} p(t)\, e^{i\xi t}\, dt \right) e^{-i\xi x}\, d\xi$$

2.4 Reduction of the contact problem to a singular integral equation

Imposition of the top surface mixed boundary condition on the slope of the normal displacement, $w_{,x}^{1} = f(x)$ in the interval $-c \le x \le c$ reduces the contact problem to the following singular integral equation where the fundamental unknown is the contact pressure

(20)

Here the term $H_{(1,1)}(\xi)$ is the first element of the inverse of the global matrix in Equation (19). The above integral is divergent because it does not vanish as the transform variable ξ approaches ± infinity. Using

the asymptotic behavior of the local and global stiffness matrices along with the Euler identity , the relation between the Fourier and Hilbert transforms, and the odd-even properties of the trigonometric functions, the singular integral equation is separated into a Cauchy-type integral and an integral with a regular kernel. The final form of these integral equations is written as

$$\frac{w^1_{,x}}{H^*_{(1,1)}} = \int_{-c}^{+c} K_0(x,t)\,p(t)\,dt + \frac{1}{\pi}\int_{-c}^{+c} \frac{p(t)}{t-x}\,dt$$

with

$$K_0(x,t) = \frac{1}{\pi}\int_0^{+\infty} \frac{H^0_{(1,1)}(\xi)}{H^*_{(1,1)}} \sin[(t-x)\xi]\,d\xi \qquad (21)$$

where $H^*_{(1,1)}$ is the first element of the inverse of the limiting global stiffness matrix [K] as ξ approaches infinity and . After the decomposition, the integrals are numerically solved by using the approach developed by Erdogan[5] that is based on the orthogonal properties of the Chebyshev polynomials.

3. NUMERICAL RESULTS

The methodology described above is applied to several representative problems using two typical piezoelectric materials: PVDF and PZT4. The properties of the materials considered in the examples are obtained from Berlincourt[8] and co-workers.

3.1 Homogeneous piezoelectric half-planes

The contact load, P, as a function of the contact half length, c, for homogeneous PVDF half-planes at different orientations is generated. The curves obtained are for angles of 0°, 15°, 30°, 45°, 60°, and 90° degrees, and are presented in Figure 2. For the case of homogeneous half-planes the solution for the contact load as a function of the contact length is given by

(22)

and the solution for the contact stress profile is described by

$$p(x) = \frac{2P}{\pi c}\left(1 - \frac{x^2}{c^2}\right)^{1/2} \qquad (23)$$

Here P represents the total load, is the contact stress, *c* is the contact half length, and is the first element of the inverse of the global matrix

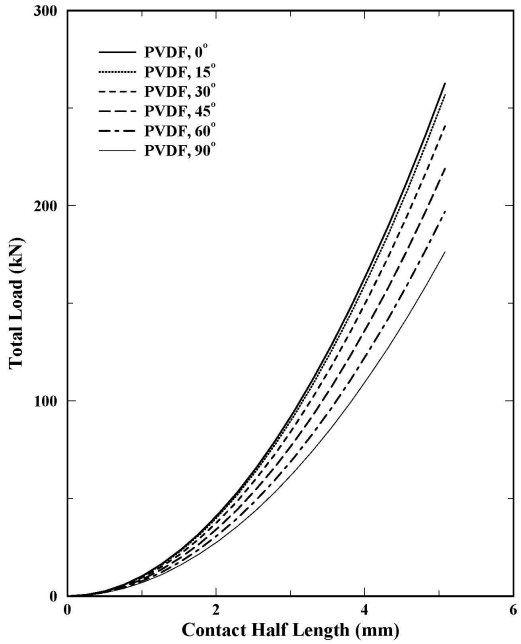

Figure 2. Total load - half length response. Homogeneous PVDF

when ξ goes to infinity. The above equations indicate that the contact load versus contact length response is parabolic, starting at zero and increasing with the size of the contact length; and the contact stress profile is elliptical and independent of the material properties. The largest magnitude of the contact pressure occurs at the center of the punch and is equal to $2/\pi$ (or 0.6366) times the value of the normalized contact pressure c/P. A value of 0.6367 is obtained for the maximum normalized contact pressure using the present approach, providing an additional check on the solution technique.

The contact load versus contact half length response curve obtained for the PZT4 homogeneous half-plane, along with the response curve of the PVDF homogeneous half-plane oriented at 0° degrees, is shown in Figure 3. It is clear that for a given contact length, the contact load force is larger for PZT4. This is primarily because the modulus of elasticity E_3 in the direction parallel to the applied load is bigger than the corresponding E_3 of the PVDF. This illustrates the same result reported by Pindera and Lane[2] where the through-the-thickness modulus of elasticity E_3 plays an important role in controlling the contact load versus contact length response.

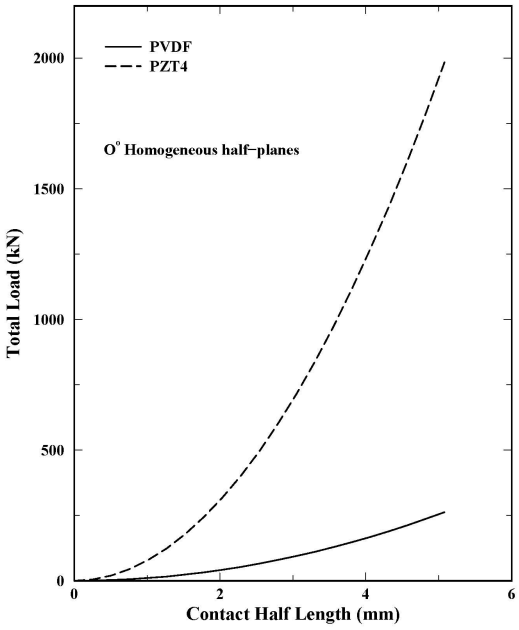

Figure 3. Total load - half length response. Homogeneous PVDF and PZT4

3.2 Piezoelectric layer embedded within an elastic medium

In general, multilayered composite laminates are typically constructed by bonding together several laminae with different material properties and fiber orientation. The resulting laminated medium can exhibit behaviors that differ from those of its constituents. We consider a composite half-plane consisting of one laminate bonded to a piezoelectric material that in turn is bonded to the half- plane. This simulates the case of a sub-surface sensing layer. The top layer and the half-plane are composed of graphite/epoxy (T300-934) and the in-between layer is either PVDF or PZT4. The thicknesses of the top layers are 0.00127 m for the graphite/epoxy and either 0.000254 m or 0.00127 m for the PVDF and PZT4. The radius of the punch is 0.0254 m. In the case of a PVDF piezoelectric layer, different off-axis angles are considered. The other plies have an orientation equal to 0° degrees. Contact load versus contact half length response curves and contact stress profiles are obtained when all these parameters are varied. The variation of the electrostatic potential that is sensed by the piezoelectric layer is also investigated.

The amount of load required to generate a given contact half length depends on the thickness of the piezoelectric layer that, in this case, plays the role of a compliant or foreign layer in the layered medium. As shown in Figure 4, the load required to generate a given contact length decreases as the thickness of the layer increases for PVDF. This results shows that the compliant layer, in this case the PVDF ply, has the effect of decreasing the overall stiffness of the multilayered medium. For the PZT4, the opposite phenomenon is observed and the load required to hold a given contact length increases as the thickness of the layer increases. In this case, the compliant layer has the effect

of increasing the stiffness of the composite laminate. The mismatch between the through-the-thickness moduli of PZT4 and graphite/epoxy is approximately 6.26 which is quite different from the case of PVDF and graphite/epoxy which is equal to 1.02. Therefore, the amount and type of variation in the response curves with respect to the change in the thickness of the compliant layer depends on the relative difference between the properties of the compliant layer and the host half-plane. The dependence on the relative difference in the through-the-thickness properties also influences the contact stress profiles as it can be seen in Figure 5. For the PVDF, there are no considerable changes since there is no practical mismatch in the through-the-thickness direction and this case is therefore not shown. In the case of PZT4, shown in Figure 5, the thicker the compliant layer yields stronger deviation of the contact stress curve from the elliptical distribution.

In Table 1, the variation of the electrostatic potential sensed by either PVDF or PZT4 within the configuration considered in this example is presented. The layer composed by PVDF senses more voltage that does the PZT4 layer. This can be explained by examining the magnitudes of the piezoelectric and dielectric constants, e_{ij} and , that are smaller in the case of PVDF. As the thickness of the piezoelectric ply increases, the electrostatic potential sensed increases as well. By looking at the constitutive equations, it can be concluded that the electrostatic potential is proportional to the thickness of the piezoelectric lamina.

Table 1. Voltage sensed by piezoelectric layer.

Material	h(mm)	Potential (kV)					
PVDF	0.254	0°	30°	45°	60°	90°	PZT4
		488.8	487.0	485.6	484.4	483.1	163.5
	1.27	1547.8	1522.8	1504.8	1487.4	1471.9	713.2

Figure 4. Total load - half length response. PVDF compliant layer

Figure 5. Contact stress profile. PZT4 compliant layer

(Contact Pressure) C/P

The change in the electrostatic potential is negligible as the off-axis angle is changed when the thickness of the piezoelectric layer is small. As this thickness is increased, the changes in the potential become more noticeable. The values for the potential are most likely out of the linear range for this type of material, and illustrate another difficulty in using the materials as pressure sensors. Figures 6 and 7 illustrate how the potential and electric displacement varies along the x-axis for the layer in consideration. As expected, it is maximum at the center and vanishes as *x* increases. In Figure 7, the change in sign of the electric displacement so that it can satisfy the equilibrium in the direction of indentation where the surface charge is equal to zero.

4. Application and conclusions

The above examples show the efficiency of the outlined technique for the study of many aspects of the contact problem of arbitrarily layered media indented by rigid punches. Numerical results can be generated to illustrate the effects of both material and geometry on the electro-mechanical response of the layered half-plane. The explicit representation of each layer by the local/global formulation has proved beneficial in the analysis of several classes of problems for layered media[2]. By extending this methodology to include piezoelectric effects and the coupled response between elastic and electric fields, new types of problems can be studied. One example includes the shape control of seat support surfaces. This is very important for persons with physical disabilities for whom effective seating and positioning are important to avoid tissue injuries due to the pressure.

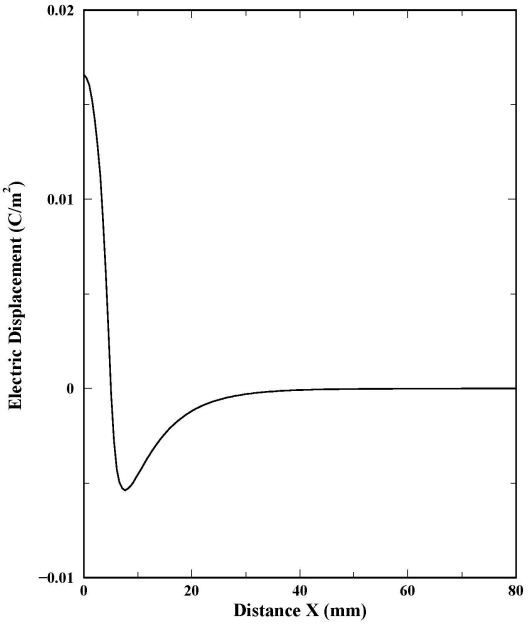

ıtion

Figure 7. Electric displacement distribution

REFERENCES

[1] Gladwell, G. M. L., *Contact Problems in the Classical Theory of Elasticity*, Sitjhoff and Noordhoff, Alphen aan den Rijn, The Netherlands, 1980.

[2] Pindera, M.-J. and M. S. Lane, "Frictionless Contact of Layered Half-Planes, Part I: Analysis", *Journal of Applied Mechanics*, **60**, 633-638, 1993.

[3] Bufler, H., "Theory of Elasticity of a Multilayered Medium", *Journal of Elasticity*, **1**,125-143, 1971.

[4] Rowe, R. K. and J. R. Booker, "Finite Layer Analysis of Nonhomogeneous Soils", *Journal of the Engineering Mechanics*, **108**,115-132, 1982.

[5] Erdogan, F., "Approximate Solutions of Systems of Singular Integral Equations", *SIAM Journal of Applied Mathematics*, **17**, 1041-1059, 1969.

[6] Heyliger, P. R. and S. P. Brooks, "Exact Solutions for Laminated Piezoelectric Plates in Cylindrical Bending", *ASME Journal of Applied Mechanics*, **63**, 903-910, 1996.

[7] Ramirez, G. and P. Heyliger, "Frictionless Contact in a Layered Piezoelectric Half-space", *Journal of Smart Materials and Structures*, **12**, 612-625, 2003.

[8] Berlincourt, D. A., D. R. Curran, and H. Jaffe, "Piezoelectric and Piezomagnetic Materials and their Function in Transformers", *Physical Acoustics*, **1**, pp. 169-270, 1964.

ACKNOWLEDGEMENTS

The discussions and assistance of Professor M.-J. Pindera of the University of Virginia are gratefully acknowledged.